

Modelling and Simulations of Ferroelectric Materials and Ferroelectric-Based Nanoelectronic Devices (Invited Paper)

D. Esseni, F. Driussi, D. Lizzit, M. Massarotto, M. Segatto.
DPIA, University of Udine, Udine, Italy

Abstract—This paper provides a brief introduction to the phenomenological aspects of the polarization in ferroelectric materials, and then an analysis of a few selected topics related to the modelling of ferroelectrics. The description of ferroelectric-based devices is quite challenging, particularly because the ferroelectric is frequently stacked with other dielectrics or with a semiconductor, as opposed to being placed between metal electrodes. Predictive modelling of ferroelectric devices is admittedly difficult, and thus the scrutiny and calibration of the models by comparison to sound experimental data is of paramount importance.

Index Terms—Ferroelectrics, modelling and simulations, polarization dynamics, FTJs, FeFETs.

I. INTRODUCTION

The discovery of ferroelectricity as a physical phenomenon dates back to about one century ago [1]. Ferroelectric materials display a spontaneous electric polarization (over some range of temperature), that can be oriented by an external electric field and lends itself to many possible nanoelectronic applications. The switchable polarization in perovskite thin films (e.g. $\text{PbZr}_{1-x}\text{Ti}_x\text{O}_3$ (PZT), $\text{SrBi}_2\text{Ta}_2\text{O}_9$ (SBT), BaTiO_3 [2]), for example, has been exploited in ferroelectric random access memories (FeRAM) since the nineties [3], [4]. Many more applications of ferroelectrics to electronic devices have been proposed after the discovery of ferroelectricity in fluorite-type $\text{Hf}_{0.5}\text{Zr}_{0.5}\text{O}_2$ [5], [6] and, more recently, in the wurtzite-type $\text{Al}_{1-x}\text{Sc}_x\text{N}$ materials [7], both materials offering a much better compatibility with CMOS processing compared to perovskites.

The exploitation of ferroelectrics in CMOS devices and circuits offers many challenges and opportunities for modelling and simulations at all abstraction levels. First principles studies are needed to clarify the phase transition paths behind the polarization switching. Physically-based, device-level models can address the stabilization and reversal of the polarization in actual devices, where ferroelectrics are stacked with other dielectrics or semiconductors. Then, compact models are also necessary to fully harness the ferroelectric properties at the circuit level.

In this paper, we will be able to touch only a few of the possible topics related to the modelling of ferroelectric materials and devices, and to provide references to deepen and widen the analysis beyond what we could address in this paper, and in the related presentation.

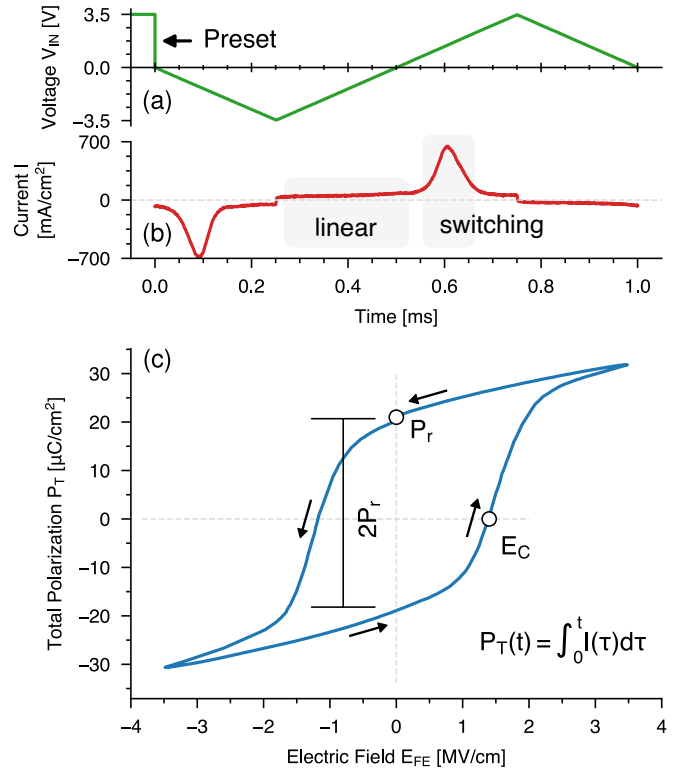


Figure 1: Electrical characterization for an MFM stack. (a) Input voltage, V_{IN} , consisting of a rectangular preset pulse followed by a triangular waveform. (b) Measured current corresponding to the V_{IN} waveform in (a). (c) Total polarization, P_T , as a function of the applied electric field. P_r and E_C denote respectively the remnant polarization and the coercive field.

II. PHENOMENOLOGICAL ASPECTS IN FERROELECTRIC MATERIALS

The total polarization P_T in a ferroelectric material can be written as $P_T = P + (\epsilon_0 \epsilon_F - 1) E_{FE}$, where E_{FE} is the electric field in the ferroelectric, ϵ_0 and ϵ_F are respectively the vacuum and background ferroelectric permittivity, and P is the spontaneous polarization. From a theoretical perspective, it has been argued that ϵ_F is more an adjustable parameter than a true material constant [8]. In thin film ferroelectrics, moreover, a contribution to ϵ_F may also stem from the coexistence of both ferroelectric and paraelectric phases in actual samples.

Metal-Ferroelectric-Metal (MFM) capacitors are the primary structures for the electrical characterization of ferroelectric materials. The polarization in an MFM stack

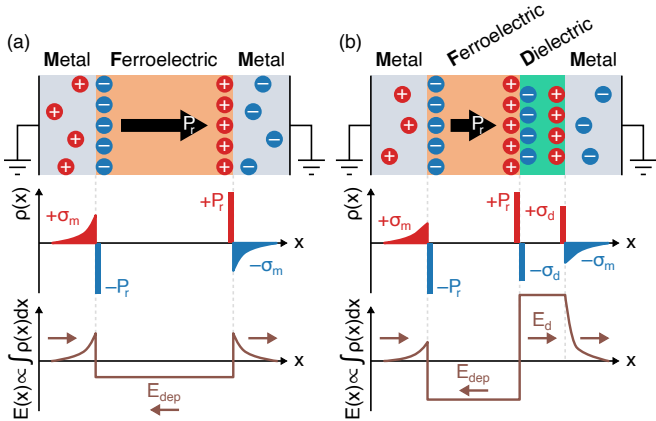


Figure 2: Sketch of the depolarization field, E_{dep} , induced by the ferroelectric polarization when it is not completely screened by ideal metal electrodes. a) MFM structure where metals have a finite screening length, hence they respond to P with a charge per unit area σ_m that is smaller than P . b) MFDM structure where P induces E_{dep} in the ferroelectric, as well as the field E_d in the dielectric.

is typically measured by applying a triangular voltage waveform V_{IN} [9], as illustrated in Fig. 1(a).

Figure 1(b) displays an example of the current, I , induced by the V_{IN} waveform in Fig. 1(a): the regions where I is fairly flat correspond to the linear dielectric response of the MFM stack, while the I peaks originate from the switching of P . Assuming that I has reached a time-periodic regime, the current is integrated over time to obtain the polarization versus field curves in Fig. 1(c).

Hafnium-based oxides exhibit P_r values between roughly 5 and 25 $\mu\text{C cm}^{-2}$ depending on the doping [10], while $\text{Al}_{1-x}\text{Sc}_x\text{N}$ can reach 100 $\mu\text{C cm}^{-2}$ [7]. These figures correspond to huge charges per unit area; in fact, we recall that 16 $\mu\text{C cm}^{-2}$ corresponds to about 10^{14} cm^{-2} electron charges. Consequently, unless the ferroelectric material is placed between two ideal metals, the polarization tends to induce an electric field in the ferroelectric and in adjacent materials, as it is illustrated in Fig. 2. The field in the ferroelectric is opposite to the polarization, therefore it is called the depolarization field.

Besides the polarization versus field curve discussed in Fig. 1(c), the polarization reversal experiments are also very important for the characterization and modelling of ferroelectrics. Polarization reversal is usually studied as a function of the applied field and pulse duration in MFM capacitors. As it can be seen in Fig. 3, the switching time drastically reduces by increasing the electric field. Two qualitatively different ferroelectric dynamics and corresponding models have been reported in the literature. The Kolmogorov-Avrami-Ishibashi (KAI) model is based on the idea that the kinetics is limited by the rate of domain propagation [13], and it describes well the polarization reversal in epitaxial materials where a single time constant is observed, as in Fig. 3(a). The Nucleation Limited Switching (NLS) regime is instead typically used for poly-crystalline materials [14], where the kinetics has a stretched exponential time dependence, stemming from

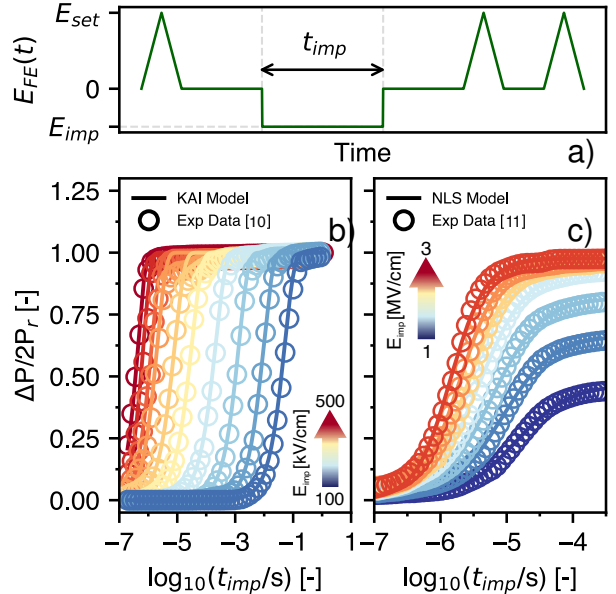


Figure 3: a) Electric Field waveform applied to the MFM stack in order to extract the polarization reversal characteristics. b) Polarization reversal curves for an epitaxial, 10 nm thick perovskite ferroelectric [11]. c) Polarization reversal curves for a 9.5 nm thick, poly-crystalline hafnium-zirconium ferroelectric [12].

many different domain nucleation times, as in Fig. 3(b).

III. MICROSCOPIC AND MACROSCOPIC MODELS

Modern physical theories define the polarization in terms of the accumulated adiabatic flow of current occurring when the crystal undergoes a deformation, and it is thus closely related to the Berry phase of the underlying Bloch functions [15]. The concept itself of macroscopic polarization, however, is intuitively linked to electric dipole moments. In a crystalline ferroelectric, the microscopic dipoles are in general due to a lack of inversion symmetry in the unit cell, as it is illustrated in Fig. 4 for BaTiO_3 . The crystal structure, polarization, dielectric as well as piezoelectric coefficients for perovskites have been long studied by using first-principles methods [16]. More recent studies have been devoted to doped HfO_2 [17], delving also into the most energetically favorable paths for polarization reversal [18], [19]. Moving to device-level modelling, the behavior of spontaneous polarization can be described with a general theory for phase transitions originally proposed by Lev Landau [21], that was later applied to ferroelectric materials [22], [23]. The model describes the equilibrium and dynamics of polarization in terms of an appropriate thermodynamic potential which, by assuming that the spontaneous polarization P lies in the z direction normal to the ferroelectric interface, we here write in the form [24], [25]

$$u_F = \alpha P^2 + \beta P^4 + \gamma P^6 - \frac{\varepsilon_0 \varepsilon_F}{2} E_{FE}^2 - E_{FE} \cdot P + k |\nabla P|^2 \quad (1)$$

where α , β and γ are the ferroelectric anisotropy coefficients, k is the domain wall coupling coefficient and ∇P

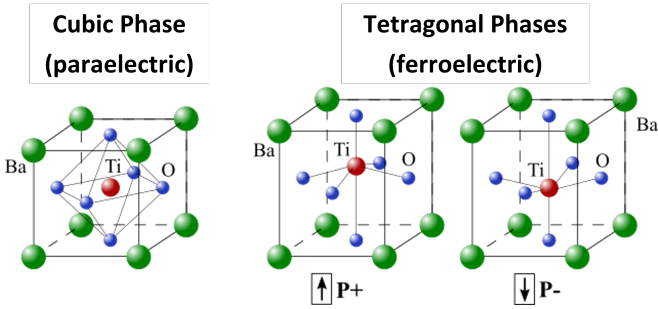


Figure 4: Sketch of the BaTiO_3 crystal cell in different phases: the cubic phase does not show any electric momentum and has a paraelectric behavior, while the tetragonal phase can appear in two different configurations with opposite electric momentum, thus showing ferroelectricity. The atom displacements are emphasized to illustrate the two ferroelectric configurations. Adapted from [20].

is the gradient of P . The always-positive, last term in Eq. (1) introduces an energy penalty for a non-uniform ferroelectric polarization pattern and, in particular, for configurations with anti-parallel adjacent dipoles.

Equation (1) neglects a possible coupling between polarization and strain, that is frequently overlooked in the analysis of electron devices, but is more relevant for applications to sensors, actuators, and energy harvesting [26], [27]. In devices where the ferroelectric is adjacent to dielectrics or semiconductors, the electrostatic energy due to the depolarization field must be included in the thermodynamic potential [24], [28]–[30]. The thermodynamic potential in the presence of conduction of free charges in the ferroelectric has been recently revisited in [25].

The Landau–Ginzburg–Devonshire (LGD) model describes the dynamics of P as [23], [31]

$$\rho \frac{\partial P}{\partial t} = -\frac{\delta U}{\delta P} = -\frac{\partial u_F}{\partial P} + 2k(\nabla^2 P) \quad (2)$$

where U is the integral of the u_F in Eq. (1) over the volume of the system, $\frac{\delta U}{\delta P}$ and $\frac{\partial u_F}{\partial P}$ respectively denote the variational derivative and the partial derivative of the functional U , and ρ is a resistivity (in $[\Omega \text{m}]$) governing the speed of the polarization dynamics. An LGD model for ferroelectrics is also available in TCAD tools [32], [33].

As already mentioned, semi-empirical equations are typically used to interpret the polarization reversal experiments in Fig. 3 [13], [14], but an analysis based on the LGD model summarized by Eqs. (1) and (2) could help us test and improve the maturity of the LGD framework.

IV. MODELLING OF FERROELECTRIC DEVICES

The modelling of ferroelectric devices is complicated by the fact that the ferroelectric can be stacked with other dielectrics or semiconductors. In the MFDM structures employed in FTJs and depicted in Fig. 5(a), for example, it has been argued that, if charge injection in the dielectric stack is not accounted for, simulation results predict P-V hysteretic curves much narrower and more tilted than their experimental counterpart [38], [39]. Hence, in these devices, the interplay between the charge trapping, the stabilization and the compensation

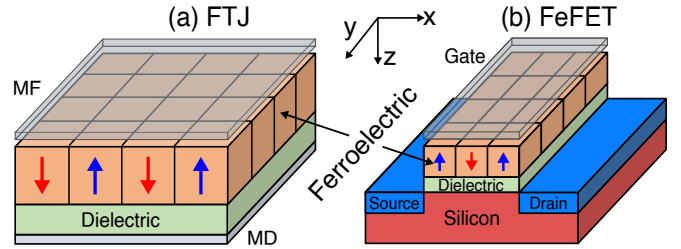


Figure 5: Examples of ferroelectric-based electron devices. a) Metal–Ferroelectric–Dielectric–Metal (MFDM) structures have been employed in Ferroelectric Tunnel Junctions (FTJs) [34]. b) Ferroelectric FET (FeFETs) can be used either as negative-capacitance FETs [28], [35], or as memories or memristive devices [36], [37].

of the ferroelectric polarization becomes quite delicate [40]. The non-hysteretic polarization switching in MFDM structures has been investigated also in the context of the negative-capacitance (NC) operation [24], [30], [41], [42], recently involving also the anti-ferroelectric ZrO_2 [43], [44].

The ferroelectric FETs (FeFETs) sketched in Fig. 5(b) have first attracted much attention as steep-slope transistors based on the ferroelectric NC behavior [28], [35], then they have been investigated for their potentials as memory or memristive devices [36], [37]. The modelling of FeFETs calls for computationally demanding three-dimensional simulations, because a description of the percolation source-to-drain current paths is essential to study a possible multi-level device operation [45].

V. OUTLOOK AND CONCLUSIONS

Ferroelectrics are CMOS-compatible active oxides with a broad set of possible applications. The polarization switching is a field-driven process that is inherently energy efficient, which is of utmost importance for memory and memristive applications. Some fundamental aspects behind the polarization reversal remain to be understood in fluorite-type $\text{Hf}_{0.5}\text{Zr}_{0.5}\text{O}_2$ and wurtzite-type $\text{Al}_{1-x}\text{Sc}_x\text{N}$ materials, and this plays a crucial role for the possibility of achieving a multi-level, quasi-analog operation of ferroelectric devices. Many challenges and opportunities still exist for the modelling of ferroelectric materials at different abstraction levels, and the modelling will play an important role in order to harness the potentials of ferroelectric materials in nanoelectronic devices and circuits.

ACKNOWLEDGMENTS

This work was supported by the European Union through the BeFerroSynaptic project (GA:871737).

REFERENCES

- [1] J. Valasek, “Piezo-Electric and Allied Phenomena in Rochelle Salt,” *Phys. Rev.*, vol. 17, pp. 475–481, Apr 1921.
- [2] K. M. Rabe, M. Dawber, C. Lichtensteiger *et al.*, *Physics of Ferroelectrics, a Modern Perspective*. Springer, 2007.
- [3] J. T. Evans and R. Womack, “An Experimental 512-bit Non-volatile Memory with Ferroelectric Storage Cell,” *IEEE Journal of Solid-State Circuits*, vol. 25, no. 5, pp. 1171–1175, 1989.
- [4] D. Takashima, “Overview of FeRAMs: Trends and Perspectives,” in *2011 11th Annual Non-Volatile Memory Technology Symposium Proceeding*, Nov 2011, pp. 1–6.

- [5] T. S. Böscke, J. Müller, D. Bräuhaus *et al.*, “Ferroelectricity in Hafnium Oxide: CMOS compatible Ferroelectric Field Effect Transistors,” in *2011 International Electron Devices Meeting*, Dec 2011, pp. 24.5.1–24.5.4.
- [6] D. Zhou, Y. Guan, M. Vopson *et al.*, “Electric Field and Temperature Scaling of Polarization Reversal in Silicon doped Hafnium Oxide Ferroelectric Thin Films,” *Acta Materialia*, vol. 99, pp. 240–246, 2015.
- [7] S. Fichtner, N. Wolff, F. Lofink *et al.*, “AlScN: A III-V Semiconductor based Ferroelectric,” *Journal of Applied Physics*, vol. 125, p. 114103, 2019.
- [8] A. P. Levanyuk, B. A. Strukov, and A. Cano, “Background Dielectric Permittivity: Material Constant or Fitting Parameter?” *Ferroelectrics*, vol. 503, no. 1, pp. 94–103, 2016.
- [9] M. Massarotto, F. Driussi, A. Affanni *et al.*, “Novel Experimental Methodologies to Reconcile Large- and Small-Signal Responses of Hafnium-based Ferroelectric Tunnel Junctions,” *Solid-State Electronics*, vol. 200, p. 108569, 2023, DOI: 10.1016/j.sse.2022.108569.
- [10] Z. Wang, J. Hur, N. Tasneem *et al.*, “Extraction of Preisach Model Parameters for Fluorite-structure Ferroelectrics and Antiferroelectrics,” *Scientific Reports*, p. 12474, 2021.
- [11] Y. W. So, D. J. Kim, T. W. Noh *et al.*, “Polarization Switching Kinetics of Epitaxial Pb(Zr_{0.4}Ti_{0.6})O₃ Thin Films,” *Applied Physics Letters*, vol. 86, no. 9, 02 2005, 092905.
- [12] D. H. Lee, G. T. Yu, J. Y. Park *et al.*, “Effect of Residual Impurities on Polarization Switching Kinetics in Atomic-Layer-Deposited Ferroelectric Hf_{0.5}Zr_{0.5}O₂ Thin Films,” *Acta Materialia*, vol. 222, p. 117405, 2022.
- [13] H. Orihara, S. Hashimoto, and Y. Ishibashi, “A Theory of D-E Hysteresis Loop Based on the Avrami Model,” *Journal of the Physical Society of Japan*, vol. 63, no. 3, pp. 1031–1035, 1994.
- [14] A. K. Tagantsev, I. Stolichnov, N. Setter *et al.*, “Non-Kolmogorov-Avrami Switching Kinetics in Ferroelectric Thin Films,” *Phys. Rev. B*, vol. 66, p. 214109, Dec 2002.
- [15] R. Resta and D. Vanderbilt, “Theory of Polarization: A Modern Approach,” in *Physics of Ferroelectrics, a Modern Perspective*, K. M. Rabe, M. Dawber, C. Lichtensteiger *et al.*, Eds. New York: Springer, 2007.
- [16] K. M. Rabe and P. Ghosez, “First-Principles Studies of Ferroelectric Oxides,” in *Physics of Ferroelectrics, a Modern Perspective*, K. M. Rabe, M. Dawber, C. Lichtensteiger *et al.*, Eds. New York: Springer, 2007.
- [17] Y. Qi and K. M. Rabe, “Phase Competition in HfO₂ with Applied Electric Field from First Principles,” *Phys. Rev. B*, vol. 102, p. 214108, Dec 2020.
- [18] H.-J. Lee, M. Lee, K. Lee *et al.*, “Scale-free Ferroelectricity Induced by Flat Phonon Bands in HfO₂,” *Science*, vol. 369, no. 6509, pp. 1343–1347, 2020, DOI: 10.1126/science.aba0067.
- [19] D.-H. Choe, S. Kim, T. Moon *et al.*, “Unexpectedly Low Barrier of Ferroelectric Switching in HfO₂ via Topological Domain Walls,” *Materials Today*, vol. 50, pp. 8–15, 2021.
- [20] K. M. Rabe, M. Dawber, C. Lichtensteiger *et al.*, “Modern Physics of Ferroelectrics: Essential Background,” in *Physics of Ferroelectrics, a Modern Perspective*, K. M. Rabe, M. Dawber, C. Lichtensteiger *et al.*, Eds. New York: Springer, 2007.
- [21] L. Landau, “On the Theory of Phase Transitions,” *Zhurnal Eksperimentalnoi i Teoreticheskoi Fiziki*, vol. 7, pp. 19–32, 1937.
- [22] A. Devonshire, “XCVI. Theory of Barium Titanate,” *The London, Edinburgh, and Dublin Philosophical Magazine and Journal of Science*, vol. 40, no. 309, pp. 1040–1063, 1949.
- [23] L. D. Landau and I. Khalatnikov, “On the Anomalous Absorption of Sound near a Second Order Phase Transition Point,” *Dokl. Akad. Nauk*, vol. 96, pp. 469–472, 1954.
- [24] T. Rollo, F. Blanchini, G. Giordano *et al.*, “Stabilization of Negative Capacitance in Ferroelectric Capacitors with and without a Metal Interlayer,” *Nanoscale*, vol. 12, pp. 6121–6129, 2020, DOI: 10.1039/C9NR09470A.
- [25] J. Bizindavyi, A. S. Verhulst, B. Sorée *et al.*, “Thermodynamic Equilibrium Theory Revealing Increased Hysteresis in Ferroelectric Field-Effect Transistors with Free Charge Accumulation,” *Communications Physics*, vol. 4, p. 86, 2021.
- [26] A. Chauhan, S. Patel, S. Wang *et al.*, “Enhanced Performance of Ferroelectric Materials under Hydrostatic Pressure,” *Journal of Applied Physics*, vol. 122, p. 224105, 2017.
- [27] Y. Li, J. Wang, and F. Li, “Intrinsic Polarization Switching in BaTiO₃ Crystal under Uniaxial Electromechanical Loading,” *Phys. Rev. B*, vol. 94, p. 184108, 2016.
- [28] S. Salahuddin and S. Datta, “Use of Negative Capacitance to Provide Voltage Amplification for Low Power Nanoscale Devices,” *Nano Letters*, vol. 8, no. 2, 2008.
- [29] M. Hoffmann, B. Max, T. Mittmann *et al.*, “Demonstration of High-speed Hysteresis-free Negative Capacitance in Ferroelectric Hf_{0.5}Zr_{0.5}O₂,” in *2018 IEEE International Electron Devices Meeting (IEDM)*, Dec 2018, pp. 31.6.1–31.6.4.
- [30] D. Esseni and R. Fontanini, “Macroscopic and Microscopic Picture of Negative Capacitance Operation in Ferroelectric Capacitors,” *Nanoscale*, vol. 13, pp. 9641–9650, 2021, DOI: 10.1039/D0NR06886A.
- [31] O. Penrose and P. C. Fife, “Thermodynamically consistent Models of Phase-Field type for the Kinetic of Phase Transitions,” *Physica D: Nonlinear Phenomena*, vol. 43, no. 1, pp. 44–62, 1990.
- [32] Synopsys Inc., *Sentaurus Device User Guide, Q-2019.12*. (Mountain View, CA: Synopsys Inc.): Synopsys Inc., 2019.
- [33] P. Lenarczyk and M. Luisier, “Physical Modeling of Ferroelectric Field-Effect Transistors in the Negative Capacitance Regime,” in *2016 International Conference on Simulation of Semiconductor Processes and Devices (SISPAD)*, Sept 2016, pp. 311–314.
- [34] B. Max, M. Hoffmann, S. Slesazek *et al.*, “Direct Correlation of Ferroelectric Properties and Memory Characteristics in Ferroelectric Tunnel Junctions,” *IEEE Journal of the Electron Devices Society*, vol. 7, pp. 1175–1181, 2019.
- [35] T. Rollo and D. Esseni, “New Design Perspective for Ferroelectric NC-FETs,” *IEEE Electron Device Letters*, vol. 39, no. 4, pp. 603–606, April 2018, DOI: 10.1109/LED.2018.2795026.
- [36] S. Slesazek and T. Mikolajick, “Nanoscale Resistive Switching Memory Devices: a Review,” *Nanotechnology*, vol. 30, no. 35, p. 352003, Jun 2019, DOI: 10.1088/1361-6528/ab2084.
- [37] H. Mulaosmanovic, S. Dinkel, J. Müller *et al.*, “Impact of Read Operation on the Performance of HfO₂-based Ferroelectric FETs,” *IEEE Electron Device Letters*, vol. 41, no. 9, pp. 1420–1423, 2020.
- [38] R. Fontanini, M. Segatto, K. S. Nair *et al.*, “Charge-Trapping-induced Compensation of the Ferroelectric Polarization in FTJs: Optimal Conditions for a Synaptic Device Operation,” *IEEE Transactions on Electron Devices*, vol. 69, no. 7, pp. 3694–3699, 2022, DOI: 10.1109/TED.2022.3175684.
- [39] M. Segatto, R. Fontanini, F. Driussi *et al.*, “Limitations to Electrical Probing of Spontaneous Polarization in Ferroelectric-Dielectric Heterostructures,” *IEEE Journal of the Electron Devices Society*, vol. 10, pp. 324–333, 2022, DOI: 10.1109/JEDS.2022.3164652.
- [40] R. Fontanini, M. Segatto, M. Massarotto *et al.*, “Modeling and Design of FTJs as Multi-Level Low Energy Memristors for Neuromorphic Computing,” *IEEE Journal of the Electron Devices Society*, vol. 9, pp. 1202–1209, 2021, DOI: 10.1109/JEDS.2021.3120200.
- [41] M. Hoffmann, F. P. G. Fengler, M. Herzig *et al.*, “Unveiling the Double-well Energy Landscape in a Ferroelectric Layer,” *Nature*, vol. 565, pp. 464–467, 2019.
- [42] M. Hoffmann, M. Gui, S. Slesazek *et al.*, “Intrinsic Nature of Negative Capacitance in Multidomain Hf_{0.5}Zr_{0.5}O₂-based Ferroelectric/Dielectric Heterostructures,” *Advanced Functional Materials*, vol. 32, no. 2, p. 2108494, 2022.
- [43] M. Hoffmann, Z. Wang, N. Tasneem *et al.*, “Antiferroelectric Negative Capacitance from a Structural Phase Transition in Zirconia,” *Nature Communications*, vol. 13, no. 1, p. 1228, Mar 2022.
- [44] M. Segatto, F. Rupil, and D. Esseni, “Analytical Procedure for the Extraction of Material Parameters in Antiferroelectric ZrO₂,” *IEEE Transactions on Electron Devices*, vol. 70, no. 6, pp. 3037–3042, 2023, DOI: 10.1109/TED.2023.3265626.
- [45] D. Lizzit, T. Bernardi, and D. Esseni, “Multi-level Operation of FeFETs Memristors: the Crucial Role of Three Dimensional Effects,” in *IEEE 52nd ESSDERC*, 2022, pp. 344–347, DOI: 10.1109/ESSDERC55479.2022.9947169.